Available online at www.sciencedirect.com

ScienceDirect

Procedia Engineering 2 (2010) 193–201

Procedia Engineering

www.elsevier.com/locate/procedia

Fatigue 2010

Fatigue behaviour of dissimilar friction stir spot weld between A6061 and SPCC welded by a scrolled groove shoulder tool

Yoshihiko Uematsu[a]*, Keiro Tokaji[a], Yasunari Tozaki[b], Yasuhito. Nakashima[c]

[a]*Gifu University, 1-1 Yanagido, Gifu 501-1193, Japan*
[b]*Gifu Prefectural Research Institute for Machinery and Material, 1288 Oze, Seki 501-3265, Japan*
[c]*ADVICS Co. Ltd., 2-1 Showa-cho, Kariya, Aichi 448-8688, Japan*

Received 2 February 2010; revised 11 March 2010; accepted 15 March 2010

Abstract

A6061 and low carbon steel sheets, SPCC, whose thicknesses were 2 mm, were welded by a friction stir spot welding (FSSW) technique using a scrolled groove shoulder tool without a probe (scroll tool). Tensile-shear fatigue tests were performed using lap-shear specimens at a stress ratio R = 0.1 in order to figure out fatigue behaviour of dissimilar welds. The tensile-shear strength of the dissimilar welds was higher than that of the A6061 similar ones. Furthermore, the dissimilar welds exhibited nearly the same fatigue strengths as the A6061 similar ones, indicating that FSSW by a scroll tool was effective technique for joining aluminium to steel sheet. The fatigue fracture modes of the dissimilar welds were dependent on load levels, where shear fracture through the interface between A6061 and steel occurred at high load levels, while a fatigue crack grew through A6061 sheet at low load levels.

Keywords: Fatigue strength; Friction stir spot welding; Dissimilar weld; Crack growth; Fracture mechanism

1. Introduction

The application of lightweight metals such as aluminium alloys in transportation industries, especially in automotive industry, is rapidly developed in order to reduce CO_2 exhaust gas and fuel consumption. However, steels are still widely used for structural components because of the lower absolute strength and higher material cost of aluminium alloys. Therefore, assembling both aluminium alloys and steels is necessary to develop hybrid body structures. It is known that fusion welding between aluminium alloy and steel are not reliable because brittle intermetallic compounds are formed along the interface [1], which results in the lower strength of welds. Recently, joining aluminium alloys to steels are tried by a friction stir welding (FSW) technique, which is a solid state welding process, and successfully achieved high strength welds [2-6].

A spot welding process using FSW technique has been newly developed, which is called friction stir spot welding (FSSW) or friction spot joining (FSJ). This method is expected to apply to joining for body parts made of aluminium sheet in transportation systems because traditional resistance spot welding of aluminium alloy usually

* Corresponding author. Tel.: +81-58-293-2501; fax: +81-58-293-2491.
E-mail address: yuematsu@gifu-u.ac.jp.

1877-7058
doi:10.1016/j.proeng.2010.03.021

results in poor reliability of joints. FSSW is a solid state joining process as well as FSW, and it is believed that FSSW is suitable for joining dissimilar metals. Consequently, FSSW was applied not only for the joining between dissimilar aluminium alloys [7, 8] but also aluminium alloy and steel. Gendo et al., for example, spot friction stir welded 6000 series aluminium alloy to zinc coated mild steel successfully [9]. Bozzi et al. joined 6008 aluminium alloy to steel and observed texture developed in the nugget [10, 11]. Furthermore, Fukumoto et al. [12-14] and Aota et al. [15] joined aluminium alloy to steel by a flat tool without probe.

For applications of FSSW to joining of load-bearing components, it is significant to elucidate the fatigue behaviour of the welds fabricated by FSSW. The authors investigated the fatigue behaviour of T4 treated Al-Mg-Si aluminium alloy welds made by FSSW [16-20] and pointed out the transition behaviour of fracture mechanism depending on load levels. Pan et al. investigated the fatigue behaviour of A6111-T4 [21-24] and A5754-O [25] welds and proposed a fatigue life estimation procedure. Wang et al. estimated the fatigue lives of A6061-T6 welds [26]. However, the fatigue behaviour of dissimilar welds between aluminium alloy and steel sheets made by FSSW has not been investigated.

In the present study, the dissimilar lap welds between aluminium alloy A6061-T6 and low carbon steel sheets, SPCC, were fabricated by FSSW technique using a newly designed scrolled groove shoulder tool without probe [27, 28] and tensile shear fatigue tests were conducted. The fatigue strengths were evaluated and the fracture mechanisms were discussed based on experimental observations of the weld zone.

2. Experimental details

2.1. Materials and specimen configuration

The materials used are A6061-T6 aluminium alloy and cold rolled low carbon steel sheets, whose thicknesses were 2 mm. The low carbon steel sheet is classified as SPCC type in Japanese Industrial Standard (JIS) G3141. The mechanical properties are listed in Table 1. The microstructures of A6061 and SPCC on the cross section are revealed in Fig.1. In A6061, the grains are elongated due to the rolling process (Fig.1 (a)), while in SPCC they are equiaxed structure (Fig.1 (b)). Fatigue and tensile specimens were made by using two 30 mm by 100 mm sheets with a 30 mm by 30 mm overlap area. The upper and lower sheets are aluminium alloy and steel, respectively. For comparison, the similar welds using two A6061-T6 sheets are also fabricated.

Table 1. Mechanical properties of materials

Material	0.2% proof stress $\sigma_{0.2}$ (MPa)	Tensile strength σ (MPa)	Elongation δ (%)	Elastic modulus E (GPa)
A6061-T6	287	311	15	67
SPCC	208	317	51	208

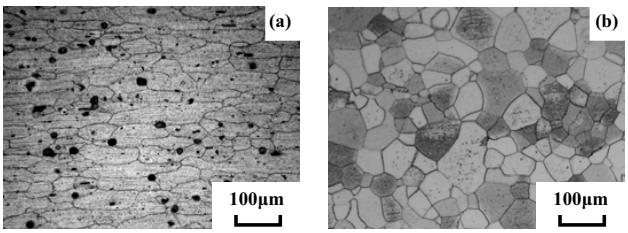

Fig. 1. Microstructures of materials on the cross section: (a) A6061-T6, (b) Steel

2.2. Tool geometry and welding conditions

A photograph of a newly designed tool is presented in Fig.2 [27, 28]. It should be noted that the tool has no probe, but a scrolled groove of 0.5 mm depth on its shoulder surface, which is referred to as the scroll tool. In FSSW, the important processing variables are the tool rotational speed, the tool holding time and the shoulder plunge depth. In this case, those variables are defined from preliminary tests and fixed as the tool rotational speeds of 3000 rpm, the tool holding times of 5 sec and the shoulder plunge depths of 1 mm. The welding variables for the A6061 similar welds are fixed as the tool rotational speeds of 3000 rpm, the tool holding times of 4 sec and the shoulder plunge depths of 1 mm, based on the other reports [27, 28]. In all cases, the plunge rate was 10 mm/min. Both sheets were polished before welding for the dissimilar welds, while surface pretreatment was not done for the similar ones.

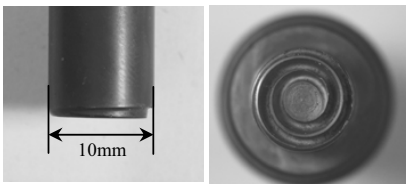

Fig. 2. Photograph showing geometry of a newly designed tool

2.3. Procedures

Fatigue tests were conducted using an electro-hydraulic fatigue testing machine operating at a sinusoidal frequency of 10 Hz and a stress ratio of $R = 0.1$. After fatigue tests, fracture surfaces were analysed in detail using a scanning electron microscope (SEM).

3. Results

3.1. Microstructure in weld zone

Figure 3 shows the top view of the specimen and the macroscopic appearances of the cross section of the weld zone in the dissimilar and similar welds. In the dissimilar weld (Fig.3 (a)), the interface between the upper and lower sheets is clearly seen, indicating that stirring of material occurred only in the upper sheet, A6061. On the contrary, the upper and lower sheets are mixed in the area inside the white dotted line in Fig.3 (b) in the similar weld. This area is defined as a mixed zone (MZ). The magnified microstructures of the areas “A”~”D” in Fig.3 (a) are revealed in Fig.4. The grains in the region inside the white dotted line in the dissimilar weld are much finer than those in the parent metal (Fig.1 (a)) due to dynamic recrystallization during welding process. The area “D” (Fig.4 (d)) is the boundary between the areas with and without grain refinement. At the interface between upper and lower sheets (Fig.4 (b), (c)), intermetallic compounds were not found by an optical microscope. In the similar weld, it was found that grain refinement took place within the MZ in Fig.3 (b).

3.2. Tensile-shear strength

The average tensile-shear strengths of three specimens in the dissimilar and similar welds are 5.4kN and 4.3kN, respectively. The fracture surface of the lower steel sheet is revealed in Fig.5. Figure 5 (b) and (c) are the magnified views at the locations indicated by the arrows “B” and “C” in Fig.5 (a). It is clear that tensile fracture occurred along the interface between the upper and lower sheets. As shown in the magnified views, elongated dimples of aluminium alloy on the steel sheet are recognized around the centre of the nugget (Fig.5 (b)), while flat surface of

the polished steel is exposed near the edge of the nugget (Fig.5 (c)). It implies that the bonding strength at the interface is higher near the centre of the nugget, where aluminium remains on the fracture surface of the lower steel sheet. In the similar weld, however, typical plug type fracture occurred.

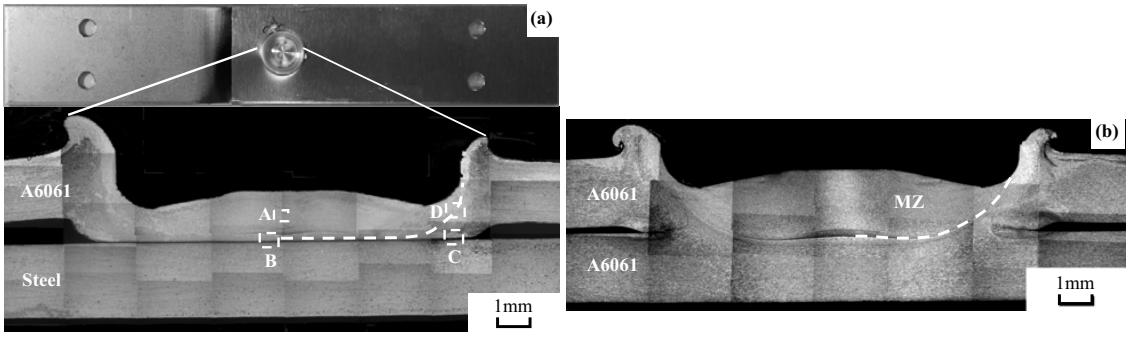

Fig. 3. Macroscopic appearance of the cross section of weld zone: (a) A6061-Steel, (b) A6061-A6061

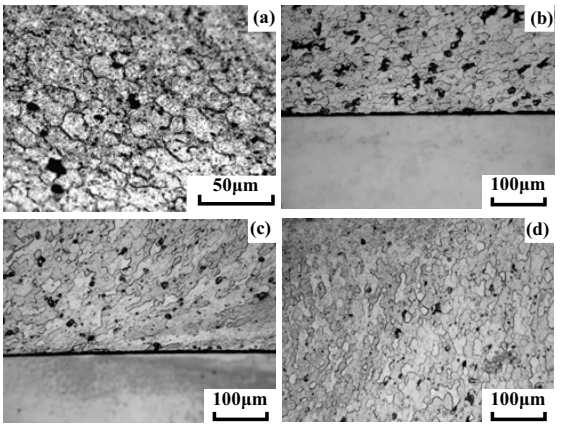

Fig. 4. Microstructures of A6061-steel dissimilar weld: (a), (b), (c), (d) Magnified views of areas “A”, “B”, “C”, “D” in Fig.3(a), respectively

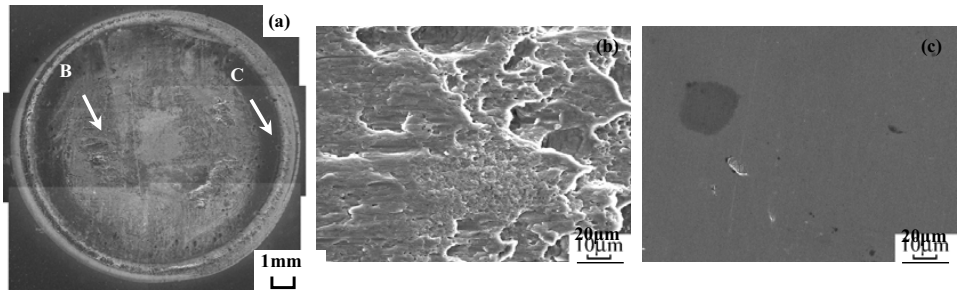

Fig. 5. SEM micrographs showing tensile fracture surface of dissimilar weld observed on the lower steel sheet: (a) Macroscopic view, (b) , (c) Magnified views at points “B” and “C” in Fig.(a), respectively. The loading direction is horizontal

3.3. Fatigue strength

Figure 6 represents the relationship between maximum load, P_{max}, and number of cycles to failure, N_f, for the dissimilar and similar welds. The test results of the friction stir spot welds fabricated by a conventional concave tool with probe are also included in the figure for comparison [17, 19]. The fatigue strengths of the similar welds made by the newly designed scroll tool are higher than those of the welds by the conventional tool with probe. The fatigue strengths of the dissimilar and similar welds by the scroll tool are nearly the same. The high tensile-shear and fatigue strengths of the dissimilar welds indicate that the scroll tool could join aluminium alloy to steel successfully.

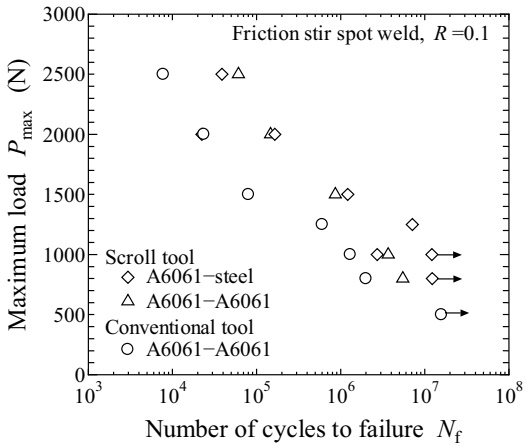

Fig. 6. Relationship between maximum load, P_{max}, and number of cycles to failure, N_f

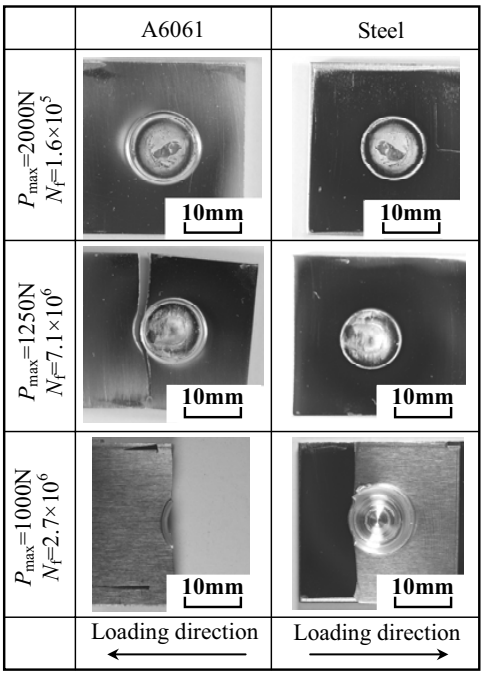

Fig. 7. Macroscopic appearance of fatigue fractured specimens in A6061-Steel dissimilar welds

3.4. Fatigue fracture morphology

Typical macroscopic appearances of fatigue-failed dissimilar welds are shown in Fig.7. When P_{max} is larger than 1250N, fatigue fracture occurred along the interface between the upper and lower sheets. This failure mode is similar to that under static loading condition (see Fig.5). At P_{max} = 1000N, however, a fatigue crack initiated in the upper aluminium sheet and grew through the upper sheet until final fracture. It should be noted that at P_{max} = 1250N, final fracture occurred along the interface, while a secondary crack grew into the upper sheet as shown in Fig.7. It indicates that the transition of fracture mechanism occurs around the maximum load of 1250N. In the similar welds, final fracture took place in the lower sheet irrelevant to load levels.

Figure 8 indicates SEM micrographs of fracture surface observed on the lower steel sheet, where P_{max} is 2000N. Figures 8 (b), (c) and (d) are the magnified views at the points “B”, “C” and “D” in Fig.8 (a), respectively. The fatigue fracture surface is seen at the point B, while static fracture surface with elongated dimples is recognized at the point C. The area in which elongated dimples are recognized is identified by the white dotted line in the figure, implying that the fatigue crack grew circumferentially around the nugget and brought about final fracture. Note that the fracture surface is very flat near the edge of the nugget (Fig.8 (d)) similar to static fracture surface, resulting from weaker bonding strength near the edge.

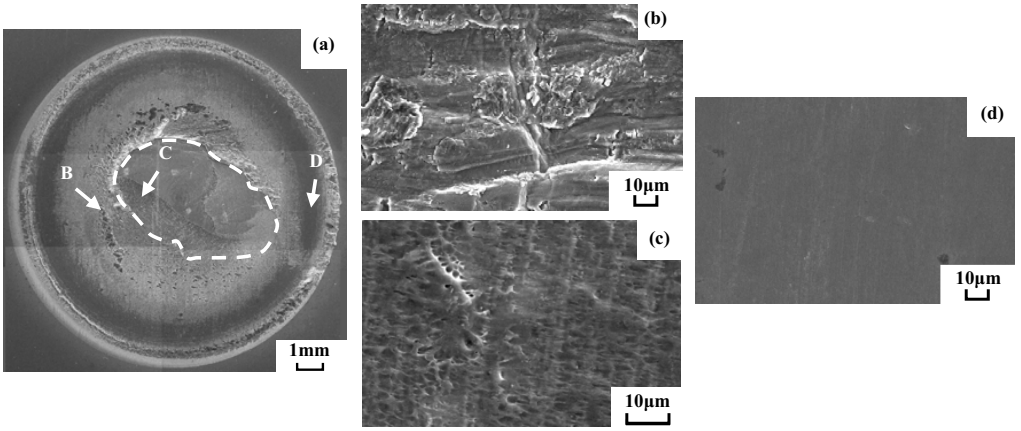

Fig. 8. SEM micrographs showing fatigue fracture surface observed on the lower steel sheet: (a) Macroscopic view, (b), (c), (d) Magnified views at points "B", "C" and "D" in Fig.(a), respectively (P_{max}=2000N , N_f=1.7×10^5). The loading direction is horizontal

Fig. 9. BEI of tensile fracture surface observed on the lower steel sheet of dissimilar weld. The loading direction is horizontal

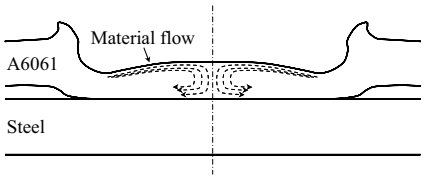

Fig. 10. Schematic illustration of material flow under the tool in dissimilar weld

4. Discussion

4.1. Tensile-shear strength

The dissimilar welds exhibited higher tensile-shear strength than the similar ones. It could be attributed to the different failure modes, where shear fracture occurred along the interface in the dissimilar welds, while plug type fracture in the similar ones. During tensile-shear test, the nugget of the similar welds could be rotated due to the specimen geometry and resulted in the plug type fracture. In the dissimilar welds, however, the stiffness of the lower steel sheet is about three times higher than that of aluminium sheet and the nugget is hardly rotated, resulting in the shear fracture along the interface.

In the previous report [19], tensile shear strengths are 2.9kN and 5.2kN for the welds fabricated by a conventional concave tool with a threaded probe and for resistance spot welds (RSW), respectively. In both welds, shear fracture through the nugget occurred. Therefore, tensile strength was normalized by the actual nugget size observed on ~~the~~ fracture surface. The normalized strengths are 123 N/mm^2 and 119 N/mm^2 for the welds made by FSSW and RSW, respectively [19]. It indicates that tensile-shear strengths are nearly the same by normalizing with respect to the actual nugget size. In the dissimilar welds, the normalized strength is calculated as 52 N/mm^2 that is much lower than those of the welds by conventional FSSW and RSW. It implies that the adhesion between the upper and lower sheets is not uniform at the interface in the nugget.

The backscattered electron image (BEI) of the fracture surface shown in Fig.5 was obtained by SEM. In a BEI, materials with different atomic weighs could be distinguished by the different contrast of the image. Figure 9 reveals the BEI of the upper part in Fig.5 (a), in which the black and white areas are identified as aluminium and steel, respectively. Then the tensile-shear strength of the dissimilar welds was normalized by the area of residual aluminium on the fracture surface of the steel sheet, namely the area of the black part in Fig.9. The normalized strength is 151 N/mm^2, which is comparable to those of the welds made by conventional FSSW and RSW. Consequently, effective adhesion between aluminium and steel is considered to be achieved in the area where aluminium remains on the static fracture surface of the steel side. Figure 9 implies that good adhesion is achieved outer circumference and near the centre of the tool. As schematically shown in Fig.10, the scroll tool induces material flow from the edge to centre and subsequently downward flow near the centre [27, 28]. It could be concluded that the downward force induced by the outer circumference of the tool and the downward flow near the centre results in the good adhesion, indicating that the downward force played important roles in the joining of the dissimilar alloys. It should be noted that the normalized strength of the dissimilar welds by the area of residual aluminium is still slightly higher than those of the welds by conventional FSSW and RSW. It is considered that the area where Fe is detected in the BEI still have adhesion, which might be weaker than the area where Al is detected.

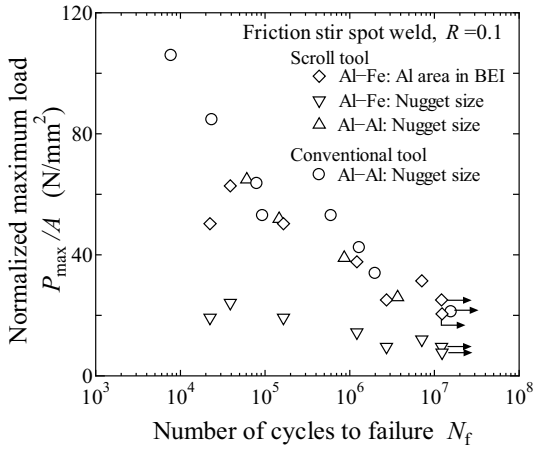

Fig. 11. Relationship between normalized maximum load, P_{max}/A, and number of cycles to failure, N_f

4.2. Fatigue behaviour

Figure 11 reveals the relationship between normalized maximum load and N_f, in which the results of the similar welds made by FSSW using a conventional concave tool with a probe are also included. The fatigue strengths of the similar welds by conventional FSSW were normalized by the actual nugget size measured on the fatigue fracture surface [17, 19]. Furthermore, the fatigue strengths of the dissimilar welds were normalized by both the nugget size measured on the fracture surface and the area of residual aluminium on the tensile fracture surface of the steel sheet. It should be noted that the fatigue failure of the similar welds made by the scroll tool occurred due to crack growth into the lower sheet. Therefore, the fatigue strengths were normalized by the nugget size measured on the cross section of the weld zone. The fatigue strengths of the dissimilar welds normalized by the nugget size are much lower than those of the other welds, while they are comparable when the fatigue strengths of the dissimilar welds are normalized by the area of residual aluminium on the steel sheet. This again indicates that the area of residual aluminium on the steel sheet could represent the effective nugget size of the dissimilar welds. It should be emphasized that the scroll grooved tool without a probe could successfully increase the effective nugget size because of the lacking of a probe and is valid for joining aluminium to steel.

5. Conclusion

Tensile and fatigue tests were performed using lap-shear specimens of the dissimilar friction stir spot welds between A6061-T6 and low carbon steel, SPCC, welded by a newly designed scrolled groove shoulder tool without probe. The results were compared with the A6061 similar welds and the fracture mechanisms were discussed based on experimental observations of the weld zone.

(1) High tensile-shear strength of the dissimilar welds was achieved by a newly designed scroll grooved tool without probe. The tensile fracture occurred through the interface between aluminium and steel.

(2) The fatigue strengths of the dissimilar welds were comparable to those of the similar ones fabricated by the scroll tool, but higher than those of the similar friction stir spot welds fabricated by a conventional concave tool with threaded probe.

(3) Fatigue fracture modes were dependent on fatigue load level, where shear fracture through the nugget occurred at high load levels and a fatigue crack grew through the aluminium sheet at low load levels.

(4) The area fraction of residual aluminium on the fracture surface of the lower steel sheet was defined from the backscattered electron image, and represented the effective nugget size of the dissimilar weld.

References

[1] Matsugi K, Wang Y, Hatayama T, Yanagisawa O, Syakagohri K. Application of electric discharge process in joining aluminum and stainless steel sheets. *J. Mater. Proc. Technol*. 2003;**135**:75-82.

[2] Fukumoto M, Tsubaki M, Shimoda Y, Yasui T. Welding between ADC12 and SS400 by means of friction stirring, *Q. J. Jpn. Weld. Soc*. 2004;**22**:309-314. [in Japanese]

[3] Chen C.M, Kovacevic R. Joining of Al 6061 alloy to AISI 1018 steel by combined effects of fusion and solid state welding. *Int. J. Mach. Tool. Manu.* 2004;**44**:1205–1214.

[4] Uzun H, Donne C.D, Argagnoto A, Ghidini T, Gambaro C. Friction stir welding of dissimilar Al 6013-T4 to X5CrNi18-10 stainless steel. *Mater. Design* 2005;**26**:41-46.

[5] Watanabe T, Takayama H, Yanagisawa A. Joining of aluminum alloy to steel by friction stir welding. *Q. J. Jpn. Weld. Soc.* 2005;**23**:186-193.

[6] Ahmed E, Takahashi M, Ikeuchi K. Friction-stir-welded lap joint of aluminium to zinc-coated steel. *J. Mater. Proc. Technol.* 2006;**178**: 342-349.

[7] Su P, Gerlich A, North T.H, Bendzsak G.J. Intermixing in dissimilar friction stir spot welds. *Metall. Mater. Trans. A* 2007;**38A**:584-595.

[8] Tran V.X, Pan J, Pan T. Effects of processing time on strength and failure modes of dissimilar spot friction welds between aluminum 5757-O and 7075-T6 sheets. *J. Mater. Proc. Technol.* 2009;**209**:3724-3739.

[9] Gendo T, Nishiguchi K, Asakawa M, Tanioka S. Spot friction welding of aluminum to steel. *SAE Technical Paper* 2007;No.2007-01-1703.

[10] Bozzi S, Etter A.L, Baudin T, Robineau A, Goussain J.C. Dynamic recrystallization mechanism on spot welding of 6008 aluminum alloy to steel by friction stir welding. *Mater. Sci. For.* 2007;**558-559**:477-483.

[11] Bozzi S, Etter A.L, Baudin T, Robineau A, Goussain J.C. Mechanical behaviour and microstructure of aluminum-steel sheets joined by FSSW. *Texture, Stress, and Micro.* 2008;ID.360617.

[12] Fukumoto M, Miyagawa K, Yasui T, Tsubaki M. Spot welding between aluminum alloy and carbon steel by friction stirring. *Proc. 6th Int. Sym. on Friction Stir Welding*, Saint-Sauveur, Canada 2006 (CD-ROM).

[13] Miyagawa K, Tsubaki M, Yasui T, Fukumoto M. Spot welding between aluminum alloy and low carbon steel by friction stirring. *Q. J. Jpn. Weld. Soc.* 2008;**26**:42-47. [in Japanese]

[14] Miyagawa K, Tsubaki M, Yasui T, Fukumoto M. Spot welding between aluminum alloy and Zn coated steel by friction stirring. *Q. J. Jpn. Weld. Soc.* 2008;**26**:131-136. [in Japanese]

[15] Aota K, Takahashi M, Ikeuchi K. Friction stir spot welding of aluminum to steel by rotating tool without probe. *Q. J. Jpn. Weld. Soc.* 26 (2008) 227-234. [in Japanese]

[16] Uematsu Y, Tokaji K, Murata S. Fatigue behaviour of friction stir spot welded joints in Al-Mg-Si alloy. *Proc. 6th Int. Sym. on Friction Stir Welding*, Saint-Sauveur, Canada 2006 (CD-ROM).

[17] Uematsu Y, Tokaji K, Murata S, Tozaki Y, Kurita T. Fatigue behaviour of friction stir spot welded Al-Mg-Si alloy. *J. Soc. of Mater. Sci., Jpn* 2007;**56**:537-543. [in Japanese]

[18] Uematsu Y, Tokaji K, Tozaki Y, Kurita T, Murata S. Effect of post heat treatment on fatigue behaviour of friction stir spot welded Al-Mg-Si alloy. *Q. J. Jpn. Weld. Soc.* 2008;**26**:7-14. [in Japanese]

[19] Uematsu Y, Tokaji K. Comparison of fatigue behaviour between resistance spot and friction stir spot welded aluminium alloy sheets. *Sci. Technol. Wel. Join.* 2009;**14**:62-71.

[20] Uematsu Y, Tokaji K, Tozaki Y, Kurita T, Murata S. Effect of re-filling probe hole on tensile failure and fatigue behaviour of friction stir spot welded joints in Al-Mg-Si alloy. *Int. J. Fat.* 2008;**30**:1956-1966.

[21] Lin P.C, Pan J, Pan T. Fracture and fatigue mechanism of spot friction welds in lap-shear specimens of aluminum 6111-T4 sheets. *SAE Technical Paper* 2005;No.2005-01-1247.

[22] Lin P.C, Pan J, Pan T. Investigation of fatigue lives of spot friction welds in lap-shear specimens of aluminum 6111-T4 sheets based on fracture mechanics. *SAE Technical Paper* 2005;No. 2005-01-1250.

[23] Lin P.C, Pan J, Pan T. Failure modes and fatigue life estimation of spot friction welds in lap-shear specimens of aluminum 6111-T4 sheets. Part 1: welds made by a concave tool. *Int. J. Fat.* 2008;**30**:74-89.

[24] Lin P.C, Pan J, Pan T. Failure modes and fatigue life estimation of spot friction welds in lap-shear specimens of aluminum 6111-T4 sheets. Part 2: welds made by a flat tool. *Int. J. Fat.* 2008;**30**:90-105.

[25] Tran V.X, Pan J, Pan T. Fatigue behavior of aluminum 5754-O and 6111-T4 spot friction welds in lap-shear specimens. *Int. J. Fat.* 2008;**30**:2175-2190.

[26] Wang D.A, Chen C.H. Fatigue lives of friction stir spot welds in aluminum 6061-T6 sheets. *J. Mater. Proc. Technol.* 2009;**209**:367-375.

[27] Tozaki Y, Uematsu Y, Tokaji K. Welding structure and tensile-shear properties of friction-stir spot welds joined by scrolled groove shoulder tool without probe in aluminium alloy. *Trans. Jpn Soc. Mech. Eng., Series A* 2009;**75**:228-234. [in Japanese]

[28] Tozaki Y, Uematsu Y, Tokaji K. A newly developed tool without probe for friction stir spot welding and its performance. *J. Mater. Proc. Technol.* Submitted.